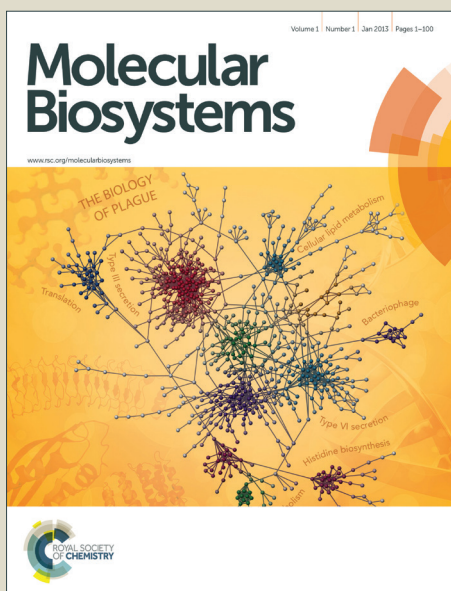


# Molecular BioSystems

Accepted Manuscript



This is an *Accepted Manuscript*, which has been through the Royal Society of Chemistry peer review process and has been accepted for publication.

*Accepted Manuscripts* are published online shortly after acceptance, before technical editing, formatting and proof reading. Using this free service, authors can make their results available to the community, in citable form, before we publish the edited article. We will replace this *Accepted Manuscript* with the edited and formatted *Advance Article* as soon as it is available.

You can find more information about *Accepted Manuscripts* in the [Information for Authors](#).

Please note that technical editing may introduce minor changes to the text and/or graphics, which may alter content. The journal's standard [Terms & Conditions](#) and the [Ethical guidelines](#) still apply. In no event shall the Royal Society of Chemistry be held responsible for any errors or omissions in this *Accepted Manuscript* or any consequences arising from the use of any information it contains.



[www.rsc.org/molecularbiosystems](http://www.rsc.org/molecularbiosystems)

# Configurational Changes of Heme Followed by Cytochrome *c* Folding Reaction

Cite this: DOI: 10.1039/x0xx00000x

Jungkweon Choi,<sup>\*,†,a</sup> Dae Won Cho,<sup>b</sup> Sachiko Tojo,<sup>a</sup> Mamoru Fujitsuka,<sup>a</sup> and Tetsuro Majima<sup>\*,a</sup>

Received 00th January 2012,  
Accepted 00th January 2012

DOI: 10.1039/x0xx00000x

www.rsc.org/

Although the folding kinetics of cytochrome *c* (Cyt-*c*), ferric or ferrous Cyt-*c*, has been extensively investigated as a paradigm for a protein folding reaction with various time-resolved spectroscopic techniques, the configurational change of heme associated with the folding reaction from a ferric Cyt-*c* to a ferrous Cyt-*c* induced by one-electron reduction has not been elucidated. To address this issue, we investigated the configurational change of heme in the Cyt-*c* folding process induced by one-electron reduction using a combination of time-resolved resonance Raman spectroscopy and pulse radiolysis. The results presented herein reveal that reduction of ferric Cyt-*c* and the ligation of Met80 occur simultaneously within a timescale of approximately 2  $\mu$ s, and that the ligand binding and exchange of heme depends on the initial configuration of the heme. The rapid ligation of Met80 observed in this study may be attributed to the intramolecular diffusion of Met80 into ferrous Cyt-*c* with a 5-coordinated high-spin configuration. Conversely, the ligand exchange of a ferrous Cyt-*c* with a 6-coordinated low-spin configuration was significantly slower.

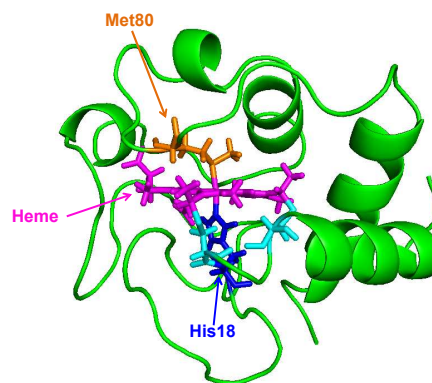
## Introduction

Conformational changes play an essential role in the biological functions of proteins, *in vivo*. Especially, the dynamics of protein folding are of particular importance in biomedical science, as accumulation of misfolded proteins can cause a variety of fatal diseases. As a result, numerous experimental and theoretical efforts have focused on understanding protein folding/unfolding processes, as summarized in recent reviews.<sup>1-5</sup>

*In vivo*, conformational changes during protein folding occur over a wide timescale (fs–s). Therefore, various time-resolved spectroscopic techniques such as time-resolved circular dichroism,<sup>6-8</sup> infrared and Raman spectroscopic techniques,<sup>9-17</sup> the fast mixing stopped-flow method,<sup>14, 18</sup> transient absorption,<sup>19-21</sup> transient grating,<sup>22-25</sup> and pulse radiolysis,<sup>26, 27</sup> have been applied to study the conformational changes that occur during protein folding reactions. Among these spectroscopic techniques, pulse radiolysis is a unique technique that has been used to trace real-time observations of the redox processes of various molecules, including protein and DNA.<sup>27-32</sup> Indeed, using pulse radiolysis technique we previously demonstrated that the oxidized form of cytochrome *c* (Cyt-*c*), ferric Cyt-*c*, is selectively reduced within a timescale of a few microseconds by an electron injection, and that the

resulting ferrous Cyt-*c* then initiates a folding reaction.<sup>26</sup> Our results indicated that the folding dynamics of Cyt-*c*, triggered by one-electron reduction, exhibited a multistep rearrangement into the native conformation.<sup>26</sup>

Although various time-resolved spectroscopic techniques have been used to investigate the folding dynamics of Cyt-*c* in the presence of a denaturant such as guanidine hydrochloride (GdHCl), the dynamics of the heme coordination states accompanied with the electron transfer-triggered folding reaction of Cyt-*c* are not yet clear. To our knowledge, here, we present the first study on the configurational changes of heme



**Scheme 1.** Solution structures of Equine heart Cyt-*c* (1GIW) retrieved from the Protein Data Bank.

accompanied with Cyt-*c* folding induced by one-electron reduction. For this study, we utilized time-resolved resonance Raman (TR<sup>3</sup>) spectroscopy combined with pulse radiolysis. TR<sup>3</sup> spectroscopy is a sensitive technique that can accurately trace the tertiary structures and structural changes of various biomolecules over a wide timescale.<sup>10, 12–14, 33</sup>

Our findings indicate that although the reduction dynamics of ferric Cyt-*c* occur within a time range of a few microseconds, the ligand binding and exchange of heme, accompanied by one-electron reduction, depends on the initial configuration of the heme. In this report, we discuss the detailed configurational changes of heme in the Cyt-*c* folding process induced by one-electron reduction.

## Results and Discussion

In native Cyt-*c*, the Fe ion of the heme coordinates axially with the His18 and Met80 residues of the Cyt-*c* protein (Scheme 1). However, upon addition of GdHCl, the bond between Met80 and the Fe ion is disrupted, resulting in denaturation of the protein. In denatured ferric Cyt-*c*, the coordination site of met80 is either occupied by a histidine (His-33 or His-26) to form a 6cLS configuration. Interestingly, previous studies have shown that while ferric Cyt-*c* is denatured in the presence of ~4 M GdHCl, ferrous Cyt-*c* remains folded under identical conditions.<sup>20, 25</sup>

To determine whether we could reproduce these findings, we measured the steady-state Raman spectra of ferric and ferrous Cyt-*c* in the presence of ~4 M GdHCl by using an excitation wavelength of 514.5 nm (Figure 1). Based on the assignments of resonance Raman spectra of Cyt-*c*, as reported by Spiro et al.<sup>15, 16</sup> and Oellerich et al.<sup>13</sup>, Raman bands for ferric and ferrous Cyt-*c* in the presence of GdHCl are assigned to those of the heme molecule, as depicted in Figure 1. The denatured ferric Cyt-*c* exhibited the characteristic  $\nu_4$  ( $\nu(\text{pyrrole half-ring})_{\text{sys}}$ ) mode at 1375 cm<sup>-1</sup>, corresponding to the porphyrin breathing mode, and the  $\nu_{10}$  ( $\nu(\text{C}_\alpha\text{C}_m)_{\text{asys}}$ ) mode at 1639 cm<sup>-1</sup>. In addition, the  $\nu_2$  ( $\nu(\text{C}_\beta\text{C}_\beta)_{\text{sys}}$ ) mode, a spin-state marker band, was observed at 1565 and 1588 cm<sup>-1</sup>, corresponding to 6-coordinated low-spin (6cLS) and 5-coordinated high-spin (5cHS) configurations, respectively.<sup>13, 14, 17</sup> Consistent with the data from previous studies,<sup>12–14, 17</sup> these data indicate that the heme moiety has a mixed configuration under denaturing conditions.

In comparison to the Raman spectrum of unfolded ferric Cyt-*c*, ferrous Cyt-*c* exhibits significantly down-shifted  $\nu_4$  and  $\nu_{10}$  vibrational modes at 1362 and 1621 cm<sup>-1</sup>, respectively, which is characteristic of the properly folded ferrous Cyt-*c*.<sup>15</sup> Indeed, the Raman spectrum of ferrous Cyt-*c* measured in ~4 M GdHCl solution is consistent with that measured in 0.5 M GdHCl solution, where both ferric and ferrous Cyt-*c* are properly folded (Figure S1). Therefore, these data support previous findings that ferrous Cyt-*c* remains folded in the presence of 3.2–4.0 M GdHCl.<sup>20, 26</sup> This result also implies that the reduction of ferric Cyt-*c* in the presence of 3.2–4.0 M GdHCl results in a conformational change to form a folded

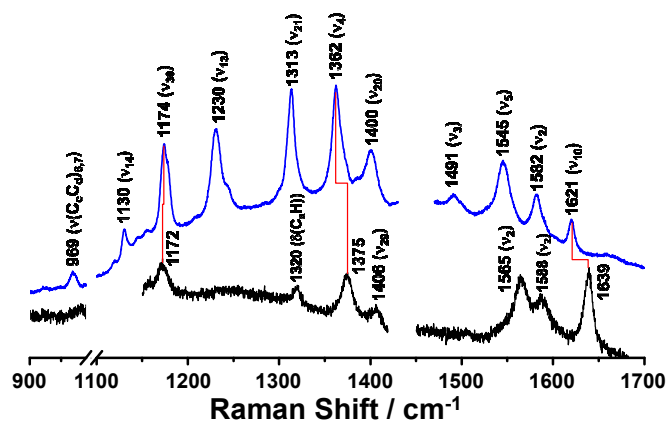


**Figure 1.** Steady-state Raman spectra of ferric Cyt-*c* (black line) and ferrous Cyt-*c* (blue line) in ~4 M GdHCl solution, respectively. ([Cyt-*c*] = 50 μM,  $\lambda_{\text{excitation}} = 514.5$  nm). The Raman spectra show that ferric Cyt-*c* is unfolded in the ~4 M GdHCl solution, whereas ferrous Cyt-*c* is folded under the same experimental conditions.

structure. Generally, the  $\nu_4$  mode is considered an indicator of the oxidation state of heme because of its sensitivity to the electron density of iron porphyrin (heme). Meanwhile, the  $\nu_{10}$  mode is sensitive to structural changes in a protein. Thus, the down-shifts in both the  $\nu_4$  and  $\nu_{10}$  modes, observed in the spectrum of ferrous Cyt-*c*, can likely be attributed to changes in both the oxidation states and in the structures of ferric and ferrous Cyt-*c* in the presence of ~4 M GdHCl. It is also noteworthy that the  $\nu_3$  ( $\nu(\text{C}_\alpha\text{C}_m)_{\text{sys}}$ ) mode is more pronounced in the spectrum of ferrous Cyt-*c* than in that of ferric Cyt-*c*, suggesting that this mode can also be used as an indicator of the folding state of Cyt-*c*.

To investigate the configurational changes of heme during the reduction-induced folding reaction of ferric Cyt-*c*, we measured the TR<sup>3</sup> spectra after pulse radiolysis of ferric Cyt-*c* in 3.5 M GdHCl. Ferric Cyt-*c*, in the presence of GdHCl, shows a strong absorption band at 409 nm (Soret band) and a weak broad band at approximately 530 nm (Q band). In contrast, the ferrous Cyt-*c* displays a strong Soret band at 417 nm and a slightly structured Q band at 500–570 nm.<sup>26</sup> Therefore, to measure the TR<sup>3</sup> spectra at the resonance wavelength, a 416-nm pulse of light was used as an excitation source. Figure 2 shows the TR<sup>3</sup> spectra obtained after pulse radiolysis of unfolded ferric Cyt-*c* in 3.5 M GdHCl. The TR<sup>3</sup> spectrum of the unfolded ferric Cyt-*c* in 3.5 M GdHCl exhibits  $\nu_4$ ,  $\nu_3$ ,  $\nu_2$ , and  $\nu_{10}$  modes at 1373, 1505, 1587, and 1639 cm<sup>-1</sup>, respectively (Figure 2). With the exception of the  $\nu_2$  mode, this spectrum is similar to the steady-state Raman spectrum for unfolded ferric Cyt-*c*. However, the intensity of some Raman signals was altered by use of the different excitation wavelength. Furthermore, the  $\nu_2$  mode at ~1585 cm<sup>-1</sup> had a very broad feature. However, peak analysis revealed that this mode actually consisted of two peaks with centre frequencies of 1564 and 1587 cm<sup>-1</sup> (Figure S2). This is consistent with the steady-state Raman spectrum of unfolded ferric Cyt-*c*. Thus, these results provide further

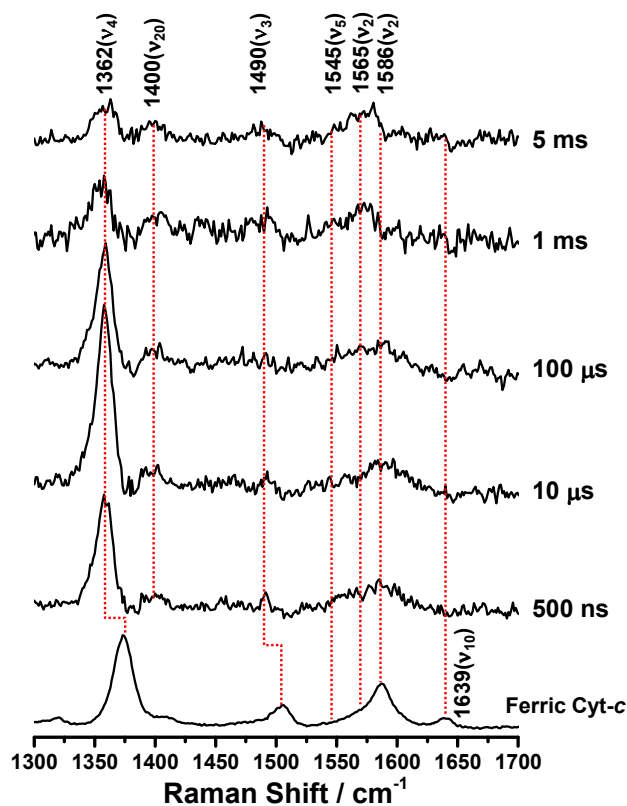


**Figure 2.** Time-resolved resonance Raman spectra obtained during pulse radiolysis of ferric Cyt-*c* in 3.5 M GdHCl. ([Cyt-*c*] = 50  $\mu$ M,  $\lambda_{\text{Excitation}}$  = 416 nm)

evidence that the 6cLS state of heme coexists with the 5cHS state under denaturing conditions, as mentioned above. According to previous studies,<sup>13, 17</sup> formation of the unfolded ferric Cyt-*c* with 6cLS configuration is mediated by His33 (or His26) and His18, whereas formation of the unfolded ferric Cyt-*c* with 5cHS configuration is coordinated by the His18 residue alone.

As depicted in Figure 2, on the other hand, the TR<sup>3</sup> spectra measured after pulse radiolysis of unfolded ferric Cyt-*c* in 3.5 M GdHCl also exhibited  $\nu_4$  and  $\nu_{20}$  modes at 1362 and 1400  $\text{cm}^{-1}$ , respectively, even in the early time-delay (e.g. at 500 ns). These  $\nu_4$  and  $\nu_{20}$  vibrations are characteristic Raman modes of ferrous Cyt-*c*. This result is therefore consistent with the proposal that we put forth in our previous study.<sup>26</sup> The unfolded ferric Cyt-*c* undergoes rapid reduction via an electron transfer from the guanidine radical formed by the fast interaction of  $e_{\text{aq}}^-$  with GdHCl. The reduced form of Cyt-*c* then structurally relaxes into an unfolded ferrous Cyt-*c* molecule. To the reduction dynamics of an unfolded ferric Cyt-*c*, we observed a time-dependent signal intensity of the  $\nu_4$  mode at 1362  $\text{cm}^{-1}$  (Figure 3). The temporal profile depicted in Figure 3 could be well fitted by a tetra-exponential function with relaxation times of  $1.4 \pm 0.9 \mu\text{s}$ ,  $5.4 \pm 4.5 \mu\text{s}$ ,  $296 \pm 30 \mu\text{s}$ , and  $>5 \text{ ms}$  (constant). These observed dynamics are similar to those reported in our previous study,<sup>26</sup> where transient absorption (TA) spectroscopy was utilized to demonstrate that the reduction of ferric Cyt-*c*

and the binding of the Met-80 residue to heme iron occur with rate constants of  $1.3 \times 10^5 \text{ s}^{-1}$  (7.7  $\mu\text{s}$ ) and  $4.3 \times 10^5 \text{ s}^{-1}$  (2.3  $\mu\text{s}$ ), respectively. These findings indicated that the reduction dynamics of ferric Cyt-*c* is slower than the ligation of Met-80 to heme.<sup>26</sup> TA spectroscopy is a useful technique for obtaining information on local protein structural changes around a chromophore. TR<sup>3</sup> spectroscopy, however, can provide detailed information about molecular vibrations by which a molecule can be chemically and structurally identified. From this point of view, the fast component of 1.4  $\mu\text{s}$ , determined by the TR<sup>3</sup> analysis, may be due to the reduction dynamics of ferric Cyt-*c* because the  $\nu_4$  mode is very sensitive to the oxidation state of heme. Consequently, one interpretation of this observation is that the reduction of ferric Cyt-*c* occurs either more rapidly than or simultaneously with the ligation of Met-80. While this interpretation is slightly different from the proposal made in our previous study<sup>26</sup>, Chen et al. found that the reduction of oxidized Cyt-*c* and the ligation of Met80 to the heme iron ( $\text{Fe}^{2+}$ ) occur simultaneously within a 5  $\mu\text{s}$  timescale.<sup>34</sup> Several other studies have reported that binding of methionine residues (Met-80 or Met-65) to the heme iron ( $\text{Fe}^{2+}$ ), followed by photodissociation of the CO ligand, takes place within a timescale of a few microseconds ( $\sim 2 \mu\text{s}$ ).<sup>6, 7, 24</sup> Furthermore, as shown in Figure 2, a new  $\nu_3$  vibrational mode at 1490  $\text{cm}^{-1}$  due to presence of ferrous Cyt-*c* with the 6cLS heme configuration was observed in the early delay time (500 ns); however, the intensity of this mode was weak. Therefore, we propose reduction of ferric Cyt-*c* and the ligation of Met80 occur simultaneously within a timescale of approximately 2  $\mu\text{s}$ . Meanwhile, that the two decay components of 5.4 and 296  $\mu\text{s}$  probably stem from conformational changes triggered by the reduction of a denatured ferric Cyt-*c* and the ligation of Met80. The slow dynamics of  $>5 \text{ ms}$  (constant) may be due to the rearrangement to the native conformation, as proposed by our prior study.<sup>26</sup>

During the folding of ferric Cyt-*c*, the ligand exchange from His18- $\text{Fe}^{3+}$ -His33 (or His18- $\text{Fe}^{3+}$ -His26; 6cLS) to His18- $\text{Fe}^{3+}$ -Met80 (6cLS) occurs via a 6-coordinate intermediate linked to a water molecule as a distal ligand. Consequently the dynamics of this reaction are very slow.<sup>11, 14</sup> Here, we consider an explanation for the rapid ligation of Met80 observed in this system. The data presented herein show that ferric Cyt-*c*, under denaturing conditions, exists in both the 6cLS and 5cHS forms,

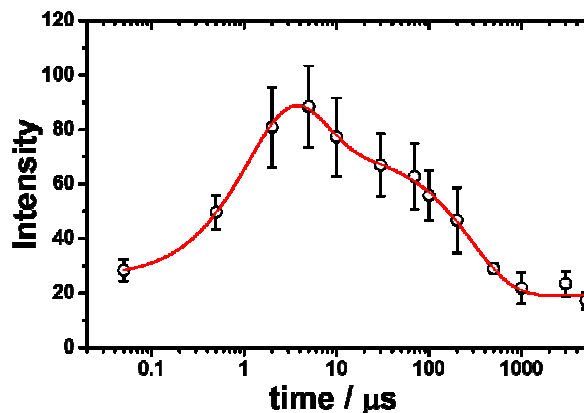


**Figure 3.** Intensity changes of the  $\nu_4$  vibrational mode at 1362  $\text{cm}^{-1}$  as a function of delay times. The theoretical fitting curve is shown in a red straight line.

as shown in Figure 1 and 2. Oellerich et al suggested that, similar to the formation of an unfolded ferric Cyt-*c*, the formation of an unfolded ferrous Cyt-*c* with a 6cLS heme might also be mediated by His-18 and His-33.<sup>13</sup> Given the folding dynamics of ferric Cyt-*c*, one would predict that the ligand exchange from His18-Fe<sup>2+</sup>-His33 (or His18-Fe<sup>2+</sup>-His26) to His18-Fe<sup>2+</sup>-Met80 during the protein folding reaction would be slow. Indeed, the  $\nu_2$  mode at 1565 cm<sup>-1</sup> of ferrous Cyt-*c*, corresponding to the 6cLS configuration, was measured with a weak intensity even in the late delay time of 5 ms, as shown in Figure 2. In contrast, the  $\nu_2$  mode of 1586 cm<sup>-1</sup>, corresponding to the 5cHS configuration of ferrous Cyt-*c*, was undetectable, suggesting a rapid ligand binding process. This result indicates that the ligand binding and exchange of heme depends on the initial coordination state of the heme molecule even though the reduction dynamics of ferric Cyt-*c* occur within a timescale of a few microseconds. Consequently, our data demonstrate that the ligand binding of ferrous Cyt-*c* with the 5cHS configuration, generated by pulse radiolysis, is relatively fast, whereas ferrous Cyt-*c* with the 6cLS configuration exhibits slow reaction dynamics. With regard to ligand exchange of unfolded ferrous Cyt-*c* with the 5cHS configuration, the ligation dynamics of Met80 are governed by the intramolecular diffusion of Met80. Abel et al. investigated the ligand rebinding dynamics that occurred after photodissociation of the CO ligand from an unfolded ferrous Cyt-*c* and proposed that the mean intramolecular diffusion times of a methionine or a histidine residue into the heme iron was  $3 \pm 2 \mu\text{s}$ ,<sup>6</sup> which is close to the speed limit of protein folding ( $\sim 1 \mu\text{s}$ ).<sup>2, 23, 35, 36</sup> This value is consistent with the results presented in this study. Thus, the fast ligation of Met80 can likely be attributed to the intramolecular diffusion of Met80 to a reduced ferrous Cyt-*c* with a 5cHS configuration.

## Conclusions

Using TR<sup>3</sup> spectroscopy combined with pulse radiolysis, we analysed the conformational changes that occurred during Cyt-*c* folding process induced by one-electron reduction. This technique provided vibrational level understanding of these protein folding and reduction processes. The reduction dynamics of ferric Cyt-*c* occurred within a timescale of a few microseconds. We also observed that the ligand binding and exchange of heme depended on its initial configuration, such as 5cHS and 6cLS. Specifically, the ligation of Met80 to a reduced ferrous Cyt-*c* with a 5cHS configuration occurs within a timescale of a few microseconds, which is close to the intramolecular diffusional time of Met80 under denaturing conditions. In contrast, a ferrous Cyt-*c* with a 6cLS configuration exhibited slow ligand-exchange dynamics.

Our results demonstrate that TR<sup>3</sup> combined with pulse radiolysis can be easily applied to study the redox reactions of various biomolecules, including protein and DNA, and can help elucidate the relationship between their structure and biological functions.

## Experimental Sections

Equine heart Cyt-*c* was purchased from Sigma-Aldrich and used without further purification.

**Pulse radiolysis.** Pulse radiolysis experiments were performed using an electron pulse (27 MeV, 11 A, 8 ns, 0.8 kGy per pulse) from a linear accelerator at Osaka University.

**Steady-state Raman** In order to clearly measure Steady-state Raman spectra, we used 514.5 nm laser line of Ar ion laser (Spectra Physics, BeamLok 2060L-S4W, 10 mW), which is a resonance wavelength. Raman signal was detected with a CCD detector (Andor Technology, DU940P-BU) equipped with a polychromator (Andor Technology, SR750-B1E).

**TR<sup>3</sup> spectroscopy.** All Cyt-*c* Solutions (100 mM phosphate buffer, pH 7.0, 50  $\mu\text{M}$  protein, and an appropriate amount of GdHCl, 3.0 ~ 4.0 M) were purged with Ar gas during the TR<sup>3</sup> measurements. The Raman experiments were performed by the flowing of sample solution through quartz capillary tube at a rate sufficient to ensure that each electron beam and laser pulse encounters a fresh sample volume. When we need accumulation to improve the signal-to-noise ratio, the sample was frequently replaced by fresh sample. The TR<sup>3</sup> spectra for Cyt-*c* after pulse radiolysis were obtained by photoexcitation with 416 nm pulse. The excitation light of 416 nm pulse is generated by the hydrogen Raman shifter of the third harmonic (355 nm) from a nanosecond Q-switched Nd:YAG laser (5-ns fwhm, Brilliant, Quantel; Les Ulis, France). The laser excitation light is synchronized with the electron pulse. The sample solution was passed through a quartz capillary tube at a slow rate sufficient to ensure that each laser pulse encountered a fresh volume of sample. The TR<sup>3</sup> spectra were collected using a polychromator (Acton, SP2500i; Trenton, NJ, USA) equipped with a charge-coupled device (CCD) camera (Princeton Instruments, PI-MAX3; Trenton, NJ, USA).

## Acknowledgements

We thank the members of the Research Laboratory for Quantum Beam Science of ISIR, Osaka University for running the linear accelerator. This work has been partly supported by a Grant-in-Aid for Scientific Research (Project 24550188, 25220806, and 25288035) from the Ministry of Education, Culture, Sports, Science and Technology (MEXT) of Japanese Government.

## Notes and references

<sup>a</sup> The Institute of Scientific and Industrial Research (SANKEN), Osaka University, Mihogaoka 8-1, Ibaraki, Osaka 567-0047, Japan.

E-mail: jkchoi@sanken.osaka-u.ac.jp, majima@sanken.osaka-u.ac.jp

<sup>b</sup> Department of Advanced Materials Chemistry, Korea University, Sejong Campus, Sejong 339-700, Korea.

<sup>†</sup> **Present Address:** Center for Nanomaterials and Chemical Reactions, Institute for Basic Science (IBS), Daejeon 305-701, Republic of Korea.

Electronic Supplementary Information (ESI) available: Experimental and supporting figures. See DOI: 10.1039/c000000x/

1. J. R. Winkler, *Curr. Opin. Chem. Biol.*, 2004, **8**, 169-174.
2. J. Kubelka, J. Hofrichter and W. A. Eaton, *Curr. Opin. Struct. Biol.*, 2004, **14**, 76-88.
3. R. L. Baldwin and G. D. Rose, *Curr. Opin. Struct. Biol.*, 2013, **23**, 4-10.
4. B. Schuler and H. Hofmann, *Curr. Opin. Struct. Biol.*, 2013, **23**, 36-47.
5. D. Thirumalai, Z. Liu, E. P. O'Brien and G. Reddy, *Curr. Opin. Struct. Biol.*, 2013, **23**, 22-29.
6. C. J. Abel, R. A. Goldbeck, R. F. Latypov, H. Roder and D. S. Kliger, *Biochemistry*, 2007, **46**, 4090-4099.
7. E. F. Chen, M. J. Wood, A. L. Fink and D. S. Kliger, *Biochemistry*, 1998, **37**, 5589-5598.
8. T. Konno, *Protein Sci.*, 1998, **7**, 975-982.
9. J. Kim, J. Park, T. Lee and M. Lim, *J. Phys. Chem. B*, 2008, **113**, 260-266.
10. M. Negrerie, S. Cianetti, M. H. Vos, J. L. Martin and S. G. Kruglik, *J. Phys. Chem. B*, 2006, **110**, 12766-12781.
11. S. R. Yeh, S. W. Han and D. L. Rousseau, *Accounts Chem. Res.*, 1998, **31**, 727-736.
12. T. Jordan, J. C. Eads and T. G. Spiro, *Protein Sci.*, 1995, **4**, 716-728.
13. S. Oellerich, H. Wackerbarth and P. Hildebrandt, *J. Phys. Chem. B*, 2002, **106**, 6566-6580.
14. S. Takahashi, S. R. Yeh, T. K. Das, C. K. Chan, D. S. Gottfried and D. L. Rousseau, *Nat. Struct. Biol.*, 1997, **4**, 44-50.
15. S. Z. Hu, I. K. Morris, J. P. Singh, K. M. Smith and T. G. Spiro, *J. Am. Chem. Soc.*, 1993, **115**, 12446-12458.
16. S. Z. Hu and T. G. Spiro, *Biophys. J.*, 1993, **64**, A157-A157.
17. E. Droghetti, S. Oellerich, P. Hildebrandt and G. Smulevich, *Biophys. J.*, 2006, **91**, 3022-3031.
18. C. K. Chan, Y. Hu, S. Takahashi, D. L. Rousseau, W. A. Eaton and J. Hofrichter, *Proc. Natl. Acad. Sci. U.S.A.*, 1997, **94**, 1779-1784.
19. J. A. Stevens, J. J. Link, Y. T. Kao, C. Zang, L. Wang and D. Zhong, *J. Phys. Chem. B*, 2010, **114**, 1498-1505.
20. T. Pascher, J. P. Chesick, J. R. Winkler and H. B. Gray, *Science*, 1996, **271**, 1558-1560.
21. S. J. Hagen, J. Hofrichter, A. Szabo and W. A. Eaton, *Proc. Natl. Acad. Sci. U.S.A.*, 1996, **93**, 11615-11617.
22. J. Choi, Y. O. Jung, J. H. Lee, C. Yang, B. Kim and H. Ihee, *ChemPhysChem*, 2008, **9**, 2708-2714.
23. J. Choi, S. Kim, T. Tachikawa, M. Fujitsuka and T. Majima, *Phys. Chem. Chem. Phys.*, 2011, **13**, 5651-5658.
24. J. Choi, C. Yang, J. Kim and H. Ihee, *J. Phys. Chem. B*, 2011, **115**, 3127-3135.
25. T. Nada and M. Terazima, *Biophys. J.*, 2003, **85**, 1876-1881.
26. J. Choi, M. Fujitsuka, S. Tojo and T. Majima, *J. Am. Chem. Soc.*, 2012, **134**, 13430-13435.
27. K. Kobayashi, H. Ue and K. Hayashi, *J. Biol. Chem.*, 1989, **264**, 7976-7980.
28. M. Fujikawa, K. Kobayashi and T. Kozawa, *J. Biol. Chem.*, 2012, **287**, 35702-35708.
29. D. C. Grills, J. A. Farrington, B. H. Layne, S. V. Lyman, B. A. Mello, J. M. Preses and J. F. Wishart, *J. Am. Chem. Soc.*, 2014.
30. K. Kawai, T. Kimura, K. Kawabata, S. Tojo and T. Majima, *J. Phys. Chem. B*, 2003, **107**, 12838-12841.
31. K. Kawai, A. Yokooji, S. Tojo and T. Majima, *Chem. Commun.*, 2003, 2840-2841.
32. K. Kawai, T. Takada, S. Tojo and T. Majima, *Tetrahedron Lett.*, 2002, **43**, 89.
33. S. R. Yeh and D. L. Rousseau, *Biophys. J.*, 1998, **74**, A128-A128.
34. E. F. Chen, P. Wittung-Stafshede and D. S. Kliger, *J. Am. Chem. Soc.*, 1999, **121**, 3811-3817.
35. I. J. Chang, J. C. Lee, J. R. Winkler and H. B. Gray, *Proc. Natl. Acad. Sci. U.S.A.*, 2003, **100**, 3838-3840.
36. K. Chattopadhyay, E. L. Elson and C. Frieden, *Proc. Natl. Acad. Sci. U.S.A.*, 2005, **102**, 2385-2389.